UDC 544.6;620.3;621.352
IRSTI 31.15.33;44.35.29

https://doi.org/10.55452/1998-6688-2026-23-3-422-433

[1,2*]Zhumadilov B.Ye.,
PhD student, ORCID ID: 0000-0001-5784-3840,
*e-mail: zhumadilovbe@gmail.com
[1,2]Markhabayeva A.A.,
PhD, ORCID ID: 0000-0002-0657-422X,
e-mail: aiko_marx@mail.ru
[1,3]Gabdullin M.T.,
PhD, ORCID ID: 0000-0003-4853-3642,
e-mail: gabdullin@physics.kz

[1]Institute of Applied Sciences and Information Technologies, Almaty, Kazakhstan
[2]Al-Farabi Kazakh National University, Almaty, Kazakhstan
[3]Kazakh-British Technical University, Almaty, Kazakhstan

RF MAGNETRON SPUTTERED WS_2 THIN FILMS ON TI AND TI/CNWS SUBSTRATES: STRUCTURAL CHARACTERIZATION AND HER PERFORMANCE

Abstract

Hydrogen evolution reaction (HER) electrocatalysts based on earth-abundant materials are promising alternatives to noble metal catalysts. In this work, WS_2 thin films were deposited on titanium substrates by RF magnetron sputtering with deposition times ranging from 30 to 120 min to investigate the influence of film thickness on structural and electrochemical properties. In addition, Ti/CNWs/WS_2 composite electrodes were fabricated by combining vertically aligned carbon nanowalls (CNWs) with a WS_2 catalytic layer. Raman spectroscopy confirmed the successful formation of multilayer WS_2 films. Electrochemical measurements revealed that HER performance strongly depends on the WS_2 deposition time. Among the investigated samples, the Ti/WS_2 electrode prepared with a deposition time of 90 min exhibited the highest catalytic activity, delivering an overpotential of 294 mV at 10 mA cm^{-2} and the lowest charge transfer resistance (R_{ct} = 15.9 Ohm) within the Ti/WS_2 series. Following electrochemical activation, the overpotential further decreased to 144 mV. Electrochemical impedance spectroscopy (EIS) showed that the incorporation of CNWs significantly enhanced charge-transfer kinetics, reducing the R_{ct} to 3.7 Ohm. However, despite the improved electron transport, the Ti/CNWs/WS_2 electrode did not outperform Ti/WS_2 in HER activity, indicating that catalytic performance depends not only on charge-transfer properties but also on the density and accessibility of active sites. These findings highlight the importance of optimizing WS_2 film thickness and electrode architecture for efficient hydrogen production.

Keywords: hydrogen evolution reaction, tungsten disulfide, RF magnetron sputtering, carbon nanowalls, electrocatalysis, electrochemical impedance spectroscopy.

Received June 26, 2026; revised August 10, 2026; accepted August 19, 2026.

Introduction

The increasing global energy demand and worsening environmental conditions require the development of sustainable and environmentally friendly energy sources. Conventional fossil fuels are major contributors to greenhouse gas emissions and climate change. Therefore, significant attention is being focused on low-carbon energy technologies, where hydrogen is considered one of the most promising and clean energy carriers [1–3].

Hydrogen is considered a highly promising energy carrier because of its high energy efficiency, environmental compatibility, and availability from diverse feedstocks. In electrochemical

energy systems, its utilization produces water as the main reaction product, minimizing harmful environmental impact. Water electrolysis is one of the most attractive approaches for sustainable hydrogen generation [4–6]. The efficiency of this technology is mainly governed by the HER, which strongly depends on the electrocatalytic performance of the electrode materials.

Precious metal-based materials, particularly platinum catalysts, are currently considered the benchmark electrocatalysts for the HER due to their excellent catalytic activity and low overpotential. However, the large-scale application of these materials is restricted by their high cost, limited availability, and poor economic feasibility for industrial use. Therefore, significant research efforts are focused on the development of low-cost and earth-abundant alternatives capable of providing high catalytic performance, long-term stability, and efficient hydrogen production [7, 8]. Layered transition metal dichalcogenides (TMDs) [9], such as MoS_2 and WS_2, are widely investigated as promising electrocatalysts for the HER in acidic media [10–13]. Their layered structure and tunable electronic properties enable the formation of numerous catalytically active sites, making these materials attractive for efficient hydrogen production. In these materials, the HER mainly occurs at the edge regions containing sulfur or metal atoms. In addition to crystalline TMDs, amorphous forms have also attracted considerable interest because their disordered structure can provide enhanced electrocatalytic activity and improved reaction performance.

Enhancement of the catalytic activity of WS_2 toward the HER is generally achieved through two main approaches: increasing the number of catalytically active sites and improving charge transfer within the material. To maximize the density of active sites, various structural engineering strategies have been employed to fabricate nanostructures with a highly developed surface area and abundant exposed edge regions. In particular, loosely stacked WS_2 nanosheets [14, 15], nanoflakes [16, 17], and WS_2/WO_3 heterostructures [18–20] have been synthesized in different studies, providing a high density of active sites and improved electrolyte accessibility to the catalyst surface. Another important strategy involves enhancing the electrical conductivity of WS_2, since its semiconducting nature limits electron transport during HER. Various approaches, including doping and the formation of composite structures, have been explored to overcome this limitation. For example, nitrogen doping has been shown to improve the intrinsic conductivity of WS_2 [21, 22], while integration with conductive graphene networks significantly accelerates charge transfer kinetics [23, 24]. In addition, flower-like WS_2 nanostructures [25, 26] demonstrated enhanced electrocatalytic performance and high stability in acidic media due to their defect-rich structure and large accessible surface area. Several studies [27–29] have also reported the deposition of WS_2 coatings by RF magnetron sputtering, which enables control of film morphology through adjustment of deposition parameters and allows observation of the transition from two-dimensional to three-dimensional structures. However, the influence of the thickness of RF-sputtered WS_2 films on the electrochemical properties of the electrodes remains insufficiently investigated.

Among carbon-based materials, carbon nanowalls (CNWs) have attracted considerable interest as promising conductive frameworks for electrochemical and electrocatalytic applications. CNWs consist of vertically aligned, interconnected graphitic nanosheets, forming an open and accessible architecture with a high density of exposed edges and defect sites. These structural features provide favorable conditions for electrolyte diffusion and increase the accessibility of surface sites, while the graphitic framework facilitates efficient electronic transport. Owing to their distinctive morphology and electrical properties, CNWs have been explored in a variety of energy-related and electrochemical applications, including supercapacitors, batteries, sensors, fuel cells, and electrocatalytic systems [30–33]. In HER electrocatalysis, CNWs can serve as conductive supports for transition metal based catalytic materials, providing an interconnected pathway for electron transport and a high surface area platform for catalyst deposition. Such a carbon framework can enhance the utilization of the active catalytic phase and facilitate electrolyte access to the electrode surface. In the present study, CNWs were employed as a conductive scaffold for WS_2 to improve interfacial charge transfer, increase the accessible surface area, and promote effective contact between the electrolyte and the

catalytic layer. The resulting Ti/CNWs/WS_2 architecture was investigated as a potential electrode configuration for enhancing the electrochemical performance toward the HER.

Therefore, the present work focuses on investigating the effect of WS_2 deposition time by RF magnetron sputtering on the structural and electrochemical properties of Ti/WS_2 and Ti/CNWs/WS_2 electrodes. RF magnetron sputtering offers several advantages, including low cost, ease of operation, high deposition rate, and scalability. Since deposition parameters strongly affect the morphology, conductivity, and catalytic activity of the coatings, their optimization is essential for the development of efficient electrodes for the HER.

Materials and methods

WS_2 thin films were deposited onto titanium foil substrates (Ti, 99.9% purity, 50 μm thickness) by RF magnetron sputtering using a HEX-L system (Korvus Technology), following a previously reported procedure [34]. Prior to RF magnetron sputtering, the titanium foils were cleaned by sequential ultrasonic treatment in acetone and isopropanol for 10 min each. This procedure was used to eliminate organic contaminants and residual impurities from the substrate surface. Following cleaning, the foils were rinsed thoroughly with distilled water, dried, and subsequently introduced into the sputtering chamber. A high-purity WS_2 target (99.9%, Kurt J. Lesker Company) was employed as the sputtering source. The deposition was carried out in an argon atmosphere with a gas flow rate of 30 sccm and a working pressure of 8.5 mTorr. The RF power was maintained at 65 W. During deposition, the substrates were heated to 250 °C and continuously rotated at 10 rpm to ensure uniform film growth. The film thickness was controlled by varying the deposition time from 30 to 120 min with a 30 min interval. Under these conditions, the deposition rate was approximately 0.24 Å s^{-1}.

Ti/CNWs/WS_2 electrodes were fabricated through a two-step process. First, vertically aligned CNWs were synthesized on titanium foil by capacitively coupled plasma-enhanced chemical vapor deposition (CCP-PECVD) according to the procedure described in our previous work [35]. Subsequently, WS_2 films were deposited onto the CNW coated substrates by RF magnetron sputtering under the same deposition conditions. As a result, a series of Ti/WS_2 and Ti/CNWs/WS_2 electrodes with different WS_2 thicknesses was obtained to investigate the effect of deposition time on the structural and electrocatalytic properties of the electrodes.

The surface morphology of the samples was characterized using a scanning electron microscope (SEM, JSM-IT210, JEOL, Japan). The structural and vibrational properties of the synthesized materials were examined by Raman spectroscopy using a Solver Spectrum NT-MDT system equipped with a 473 nm excitation laser.

Electrochemical characterization was performed at room temperature using a Metrohm potentiostat in a conventional three-electrode configuration. An Ag/AgCl electrode containing 3 M KCl served as the reference electrode, while a platinum mesh was used as the counter electrode. The prepared Ti/WS_2 and Ti/CNWs/WS_2 samples were employed as working electrodes. All measured potentials were converted to the reversible hydrogen electrode (RHE) scale according to the Nernst equation. The electrocatalytic performance toward the HER was evaluated by cyclic voltammetry (CV) and linear sweep voltammetry (LSV) in 0.5 M H_2SO_4 (pH ≈ 0.71). Measurements were carried out over a potential range from 0.2 to -0.36 V versus RHE at a scan rate of 10 mV s^{-1}. The geometric surface area of each working electrode was 1 cm^2. Electrochemical activation was performed by CV in the potential range from 0.20 to -0.36 V at a scan rate of 50 mV s^{-1} for 50 cycles. EIS measurements were conducted at -0.23 V versus RHE over a frequency range from 100 kHz to 0.1 Hz using an AC perturbation amplitude of 10 mV. The R_{ct} was determined by fitting the experimental Nyquist plots.

Results and discussion

SEM images of the Ti/CNWs and Ti/CNWs/WS_2 electrodes after 90 min of WS_2 deposition are shown in Figure 1a,b, respectively. The Ti/CNWs electrode exhibits a dense network of vertically oriented and interconnected carbon nanowalls, resulting in a rough and highly textured surface. The

open structure of the CNW network provides a large accessible surface area and serves as an effective scaffold for the subsequent deposition of the WS_2 catalytic layer. After 90 min of WS_2 deposition, the surface morphology of the Ti/CNWs/WS_2 electrode changes noticeably. The surface appears more textured and relatively uniformly covered, while the characteristic vertically oriented CNW framework remains distinguishable. These morphological features suggest the successful formation and deposition of a WS_2 layer over the CNW network.

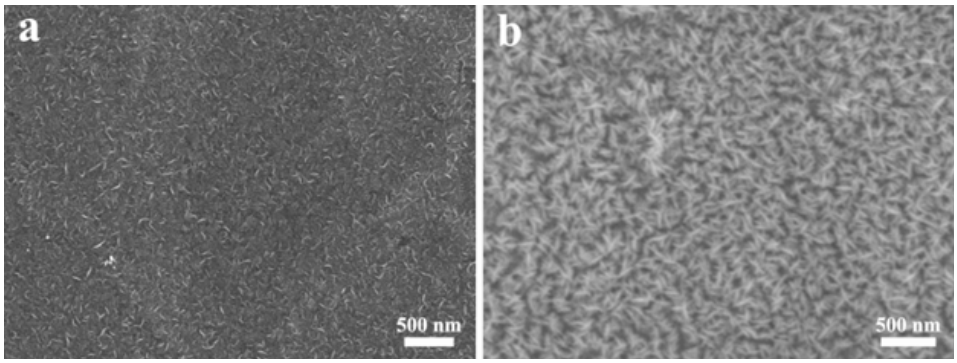

Figure 1 – SEM surface images of (a) Ti/CNWs
and (b) Ti/CNWs/WS_2 electrodes with a WS_2 deposition time of 90 min

Figure 2a,b presents the Raman spectra of Ti/WS_2 electrodes deposited for different sputtering times (30-120 min) and Ti/CNWs/WS_2 electrode. For all Ti/WS_2 samples, characteristic Raman peaks located at approximately 351.4 cm^{-1} and 417.1 cm^{-1} were observed, corresponding to the E^1_{2g} and A_{1g} vibrational modes, respectively [36, 37]. The E^1_{2g} mode is associated with the in-plane vibrations of W and S atoms, whereas the A_{1g} mode originates from the out-of-plane vibrations of sulfur atoms perpendicular to the WS_2 layers. The frequency difference between these two modes is 65.7 cm^{-1}, which is characteristic of multilayer WS_2 structures and is in good agreement with previously reported values for WS_2 thin films [38].

In addition to the characteristic WS_2 modes, weak Raman bands were detected at approximately 520.1 cm^{-1} and 560.4 cm^{-1}. These peaks may be attributed to tungsten oxide species (WO_x) formed due to partial surface oxidation of WS_2 upon exposure to air, or to second-order Raman scattering processes [39, 40]. The relatively low intensity of these bands indicates that WS_2 remains the dominant phase in the deposited films. No additional impurity related peaks were observed, confirming the successful formation of WS_2 films on titanium substrates by magnetron sputtering and indicating the high phase purity of the deposited coatings.

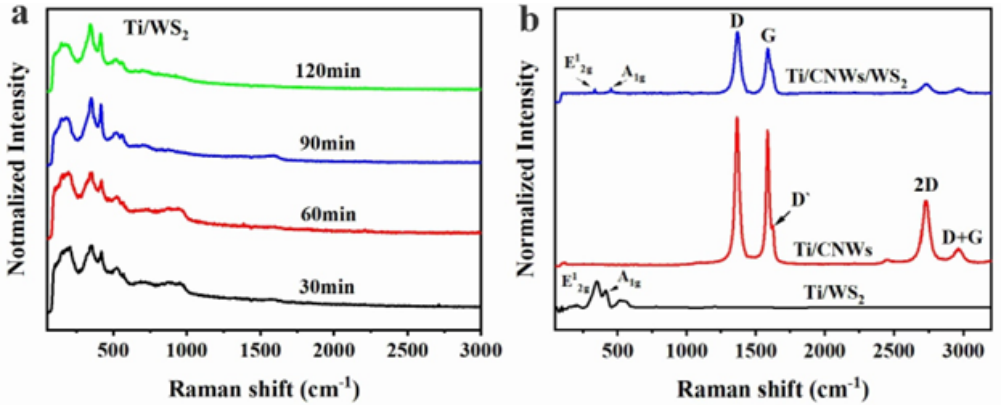

Figure 2 – Raman spectra of Ti/WS_2 and Ti/CNWs/WS_2 electrodes:
(a) effect of WS_2 deposition time on the structure of Ti/WS_2 films;
(b) comparison of Ti/WS_2, Ti/CNWs, and Ti/CNWs/WS_2 electrodes
with a WS_2 deposition time of 90 min

A noticeable modification of the Raman spectrum was observed for the Ti/CNWs/WS_2 electrode (Figure 2b). The characteristic WS_2 modes were shifted to 333.8 cm^{-1} and 452.3 cm^{-1} compared to those of the Ti/WS_2 samples. Such shifts may be attributed to interfacial interactions between WS_2 and CNWs, which can affect the local crystal structure and vibrational properties of the material. The substantial shift of the high-frequency mode toward higher wavenumbers suggests possible changes in the local bonding environment of sulfur atoms, as well as charge redistribution at the CNWs/WS_2 interface.

The Raman spectra of the Ti/CNWs and Ti/CNWs/WS_2 electrodes exhibit characteristic bands associated with graphitized carbon materials. The D band, located at approximately 1364.7 cm^{-1}, is attributed to structural defects, vacancies, crystallite boundaries, and edge sites within the carbon lattice. The G band at 1585.4 cm^{-1} corresponds to the vibrational mode of sp^2-hybridized carbon atoms and indicates the formation of a graphitic structure [41, 42]. The D′ band observed at around 1621.4 cm^{-1} is also related to defects in the sp^2 carbon network and reflects the presence of structural disorder. The 2D band at 2728.1 cm^{-1} represents the second-order overtone of the D band and is a characteristic feature of graphene-like carbon structures. In addition, the D+G band located at approximately 2963.1 cm^{-1} originates from two-phonon scattering processes and is commonly observed in defective graphitized carbon materials. The I_D/I_G ratio increased from 1.09 for Ti/CNWs to 1.37 after the deposition of WS_2. This increase indicates a higher degree of structural disorder and a greater contribution of defect-related sites in the carbon framework. The observed change in the Raman response suggests that the formation of the WS_2 layer affects the local structural environment of the CNWs.

The electrocatalytic activity of the fabricated electrodes toward the HER was investigated by CV and LSV. The obtained results are presented in Figure 3a,b.

Analysis of the CV curves (Figure 3a) reveals that all Ti/WS_2 electrodes exhibit significantly higher cathodic current densities compared to the bare Ti substrate, unambiguously confirming the catalytic contribution of the deposited WS_2 layer to the HER process. The observed systematic increase in cathodic current density with increasing deposition time from 30 to 90 min indicates a progressive enhancement in the concentration of electrochemically active sites responsible for proton adsorption and reduction. The Ti/WS_2 (90 min) electrode demonstrates the highest cathodic current density among the entire series of investigated samples, reflecting the most favorable HER kinetics and superior catalytic activity.

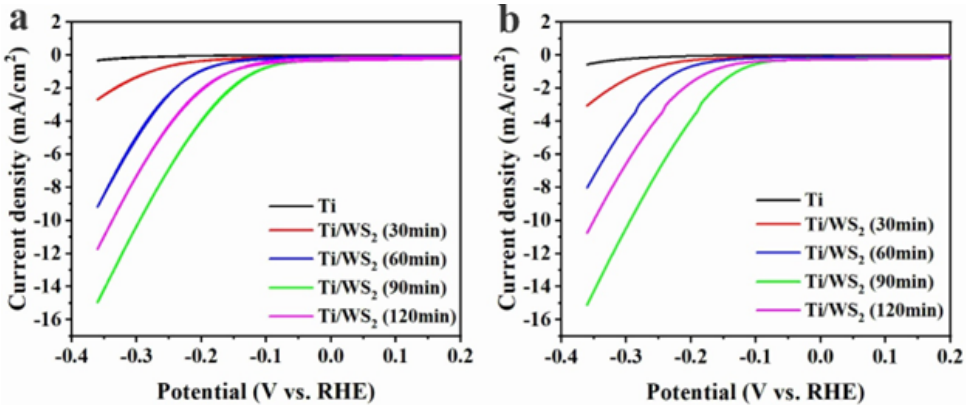

Figure 3 – Electrochemical characterization of Ti/WS_2 electrodes prepared with different WS_2 deposition times (30-120 min): (a) CV and (b) LSV curves

However, a further increase in deposition time to 120 min results in a decrease in cathodic current density, which may be attributed to the formation of an excessively thick catalytic film that impedes interfacial charge transfer and restricts the accessibility of catalytically active edge sites of WS_2 to the reactants.

The LSV results (Figure 3b) are consistent with the CV data and further corroborate the electrocatalytic performance of the Ti/WS_2 (90 min) electrode. The overpotential required to achieve a current density of 10 mA·cm^{-2} for this electrode was determined to be 294 mV, representing the lowest value among all investigated Ti/WS_2 samples and confirming its enhanced HER activity. The improved electrocatalytic performance of the Ti/WS_2 (90 min) electrode can be rationalized by the optimal catalytic film thickness, which provides the maximum number of accessible active sites while simultaneously maintaining efficient electron transport within the catalyst layer and Ti. Taken together, the electrochemical measurements demonstrate that the HER catalytic activity of Ti/WS_2 electrodes is governed by the WS_2 deposition time, with 90 min representing the optimal deposition duration within the scope of the present study.

The charge transfer kinetics at the electrode/electrolyte interface were investigated by EIS at an applied potential of -0.23 V. The Nyquist plots are presented in Figure 4. The EIS spectra were fitted using an R_s-(R_{ct}||CPE) equivalent circuit.

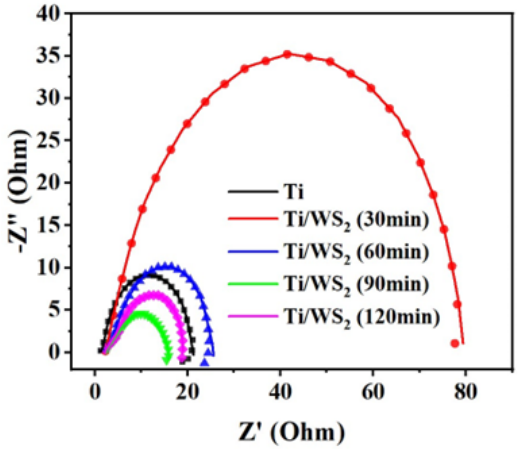

Figure 4 – Nyquist plots of Ti and Ti/WS_2 electrodes prepared with different WS_2 deposition times (30-120 min), recorded in 0.5 M H_2SO_4 at -0.23 V vs. RHE, the solid lines represent the fitted curves

The obtained R_{ct} values decrease monotonically with increasing deposition time from 30 to 90 min (78.2-15.9 Ohm), followed by a slight increase to 18.9 Ohm for the 120 min sample. The bare Ti substrate yielded an R_{ct} value of 21.2 Ohm. The markedly elevated R_{ct} observed for the Ti/WS_2 (30 min) electrode is indicative of incomplete surface coverage and an insufficient density of active catalytic sites at the early stage of deposition. The progressive decrease in R_{ct} with increasing deposition time up to 90 min reflects the formation of a continuous, highly conductive WS_2 layer with an enhanced density of active sites. The moderate increase in R_{ct} for the 120 min sample relative to the optimal 90 min electrode may be attributed to excessive film thickness, which restricts electron transport through the catalyst layer and reduces the accessibility of the active edge sites of WS_2.

The minimum R_{ct} value of 15.9 Ohm recorded for the Ti/WS_2 (90 min) electrode is consistent with its superior performance in CV and LSV measurements, confirming that a deposition time of 90 min represents the optimal condition, providing the most favorable balance among film thickness, electrical conductivity, and active site density.

Based on the optimal WS_2 deposition time of 90 min established for the Ti/WS_2 series, the same deposition duration was employed for the fabrication of the Ti/CNWs/WS_2 composite electrode. The introduction of an intermediate CNWs layer between the Ti substrate and the WS_2 catalytic layer was intended to increase the effective surface area and provide a conductive network facilitating charge transport.

The electrocatalytic performance of the Ti/CNWs/WS_2 electrode was evaluated in comparison with the optimized Ti/WS_2 electrode and the bare Ti substrate using CV and LSV before and after electrochemical activation. The corresponding results are presented in Figure 5a,b.

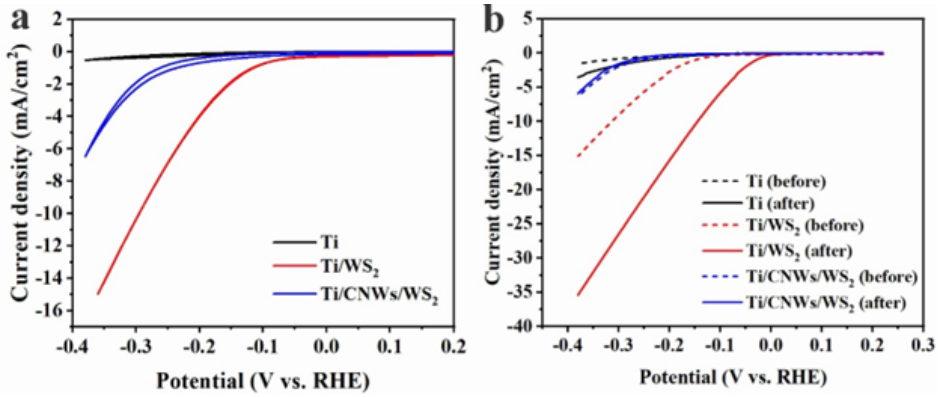

Figure 5 – Electrochemical characterization of Ti, Ti/WS_2, and Ti/CNWs/WS_2 electrodes: (a) CV and (b) LSV curves

The CV curves (Figure 5a) reveal that the Ti/WS_2 electrode exhibits the highest cathodic current density among all investigated samples, whereas the Ti/CNWs/WS_2 electrode shows a less pronounced cathodic response. This observation suggests that direct deposition of WS_2 onto the Ti substrate results in a higher density of electrochemically accessible active sites compared to the CNWs based architecture.

The LSV curves recorded before and after electrochemical activation (Figure 5b) demonstrate a significant improvement in HER performance for all electrodes following the activation procedure. For the Ti/WS_2 electrode, the overpotential required to achieve a current density of 10 mA cm^{-2} decreases from 314 to 144 mV after activation, representing the best performance among the investigated samples. The enhanced activity is attributed to electrochemical surface restructuring of WS_2, removal of surface contaminants, and increased accessibility of catalytically active sites. In contrast, the bare Ti substrate exhibits negligible HER activity both before and after activation, confirming that the observed catalytic performance originates from the WS_2 layer.

To further evaluate the HER kinetics, Tafel plots were derived from the LSV polarization curves recorded after electrochemical activation (Figure 6a). The Tafel slopes of Ti, Ti/WS_2, and Ti/CNWs/WS_2 were 207.6, 59.4, and 125.7 mV/dec, respectively. Among the investigated electrodes, Ti/WS_2 exhibited the lowest Tafel slope, indicating the most favorable HER kinetics. Although Ti/CNWs/WS_2 showed significantly lower charge transfer resistance, its higher Tafel slope suggests slower reaction kinetics. This indicates that HER performance depends not only on charge transfer efficiency but also on the number and accessibility of catalytically active sites. The high Tafel slope of the bare Ti substrate confirms its poor intrinsic HER activity.

The charge transfer kinetics of Ti, Ti/WS_2, and Ti/CNWs/WS_2 electrodes were further investigated by EIS, and the corresponding Nyquist plots are presented in Figure 6b. The R_{ct} values were determined to be 21.2 Ohm for bare Ti, 15.8 Ohm for Ti/WS_2, and 3.7 Ohm for Ti/CNWs/WS_2.

The lowest R_{ct} value obtained for Ti/CNWs/WS_2 indicates substantially enhanced interfacial charge transfer kinetics. Compared with Ti/WS_2 and bare Ti, the R_{ct} decreases by factors of 4.3 and 5.7, respectively. This improvement can be attributed to the highly conductive CNWs network, which provides efficient electron transport pathways between the Ti substrate and the WS_2 catalytic layer.

Despite exhibiting the lowest R_{ct} value, the Ti/CNWs/WS_2 electrode does not outperform Ti/WS_2 in terms of cathodic current density and HER overpotential. This result indicates that HER activity is governed not only by charge transfer kinetics but also by the density and accessibility of catalytically active sites. The presence of the CNWs interlayer may influence the morphology and distribution of the deposited WS_2, thereby reducing the number of exposed edge sites known to be responsible for HER activity. Furthermore, the three-dimensional CNWs architecture may introduce additional proton diffusion limitations within the catalytic layer. Consequently, although the CNWs interlayer significantly improves electron transport, these factors limit the overall electrocatalytic performance

of the Ti/CNWs/WS_2 electrode. Further optimization of CNWs morphology and WS_2 deposition conditions may enable more effective utilization of the advantages offered by this hybrid electrode architecture.

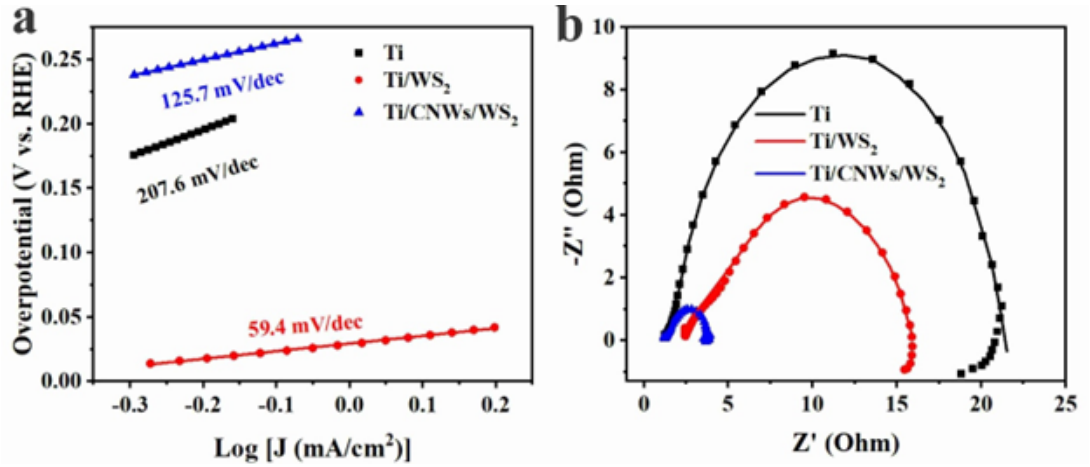

Figure 6 – (a) Tafel slope of Ti, Ti/WS_2, and Ti/CNWs/WS_2 electrodes;
(b) Nyquist plots of Ti, Ti/WS_2, and Ti/CNWs/WS_2 electrodes
recorded in 0.5 M H_2SO_4 at -0.23 V vs. RHE, the solid lines represent the fitted curves

Conclusion

WS_2 thin-film electrocatalysts were successfully fabricated on titanium substrates by RF magnetron sputtering with deposition times ranging from 30 to 120 min. Raman spectroscopy confirmed the formation of multilayer WS_2 coatings with characteristic E^1_{2g} and A_{1g} vibrational modes. The electrocatalytic performance toward the HER was found to be strongly dependent on the deposition time. Among the investigated samples, the Ti/WS_2 electrode prepared with a deposition time of 90 min exhibited the best HER performance, characterized by the highest cathodic current density, the lowest overpotential of 294 mV at 10 mA cm^{-2}, and the minimum R_{ct} of 15.9 Ohm within the Ti/WS_2 series. Electrochemical activation further improved the catalytic activity, reducing the overpotential to 144 mV.

The incorporation of a carbon nanowall interlayer resulted in a significant decrease in R_{ct} to 3.7 Ohm, demonstrating the beneficial role of CNWs in facilitating electron transport. Nevertheless, the Ti/CNWs/WS_2 electrode showed lower HER activity than the optimized Ti/WS_2 electrode, indicating that enhanced electrical conductivity alone is insufficient to maximize catalytic performance. The results suggest that the density and accessibility of catalytically active WS_2 edge sites play a dominant role in determining HER activity.

Overall, the study demonstrates that RF magnetron sputtering is an effective method for the fabrication of WS_2 based HER electrocatalysts and highlights the importance of optimizing film thickness and electrode architecture. These findings provide useful guidelines for the development of efficient, low-cost, and scalable WS_2 based electrodes for sustainable hydrogen production. Future work will involve systematic optimization of the CNWs height to determine its effect on the electrochemical and electrocatalytic performance of Ti/CNWs/WS_2 electrodes.

Information on funding. This research has been funded by the Ministry of Science and Higher Education of the Republic of Kazakhstan (Grant No. BR28712419).

REFERENCES

1 Nelson, C., Gui, M.M., and Robertson, P.K.J. The Environmental Emission and Climate Change Impact of Hydrogen Fuel Derived from Photocatalysis Water-Splitting Reaction. Advanced Energy and Sustainability Research, 6 (5) (2025). https://doi.org/10.1002/aesr.202400337.

2 Tiwari, A. Hydrogen Leading the Green Energy Future. Advanced Materials Letters, 13 (2), 2202–1690 (2022). https://doi.org/10.5185/amlett.2022.021690.

3 Wang, X., Zhou, W., Wang, Y., Gong, L., Liu, X., and Zhou, X. MoO2/Mo heterostructures for hydrogen evolution reaction and ammonia sensing in self-powered mode. Nano Energy, 109, 108253 (2023). https://doi.org/10.1016/j.nanoen.2023.108253.

4 Boretti, A., and Pollet, B.G. Hydrogen economy: Paving the path to a sustainable, low-carbon future. International Journal of Hydrogen Energy, 93, 307–19 (2024). https://doi.org/10.1016/j.ijhydene.2024.10.350.

5 Shaterabadi, M., Sadeghi, S., and Jirdehi, M.A. The Role of Green Hydrogen in Achieving Low and Net-Zero Carbon Emissions: Climate Change and Global Warming. pp. 141–53 (2024). https://doi.org/10.1007/978-3-031-52429-5_6.

6 Kalkozova, Zh.K., Markhabayeva, A.A., Mukhametkarimov, Y.S., Yerlanuly, Y., Tulegenova, A.T., Abdullin, Kh.A., Nuraje, N., and Cao, C.D. PHOTOELECTROCHEMICAL PROPERTIES OF NANOSTRUCTURED SILICON FOR SOLAR WATER SPLITTING. Herald of the Kazakh-British technical university, 21 (4), 245–53 (2024). https://doi.org/10.55452/1998-6688-2024-21-4-245-253.

7 He, H., Mai, J., Hu, K., Yu, H., Zhang, Z., Zhan, F., and Liu, X. Recent advances in electrocatalysts for efficient hydrogen evolution reaction. Rare Metals, 44 (4), 2208–38 (2025). https://doi.org/10.1007/s12598-024-02649-1.

8 Kim, J., Jung, S., Lee, N., Kim, K., Kim, Y., and Kim, J.K. Efficient Alkaline Hydrogen Evolution Reaction Using Superaerophobic Ni Nanoarrays with Accelerated H_2 Bubble Release. Advanced Materials, 35 (52) (2023). https://doi.org/10.1002/adma.202305844.

9 Bozheyev, F., Nemkayeva, R., Yerlanuly, Y., Gabdullin, M., and Markhabayeva, A. Performance of Transition Metal Oxides for Solar Hydrogen Conversion. ACS Catalysis, 15 (18), 16449–62 (2025). https://doi.org/10.1021/acscatal.5c03869.

10 Huang, T.-X., Cong, X., Wu, S.-S., Wu, J.-B., Bao, Y.-F., Cao, M.-F., Wu, L., Lin, M.-L., Wang, X., Tan, P.-H., and Ren, B. Visualizing the structural evolution of individual active sites in MoS2 during electrocatalytic hydrogen evolution reaction. Nature Catalysis, 7 (6), 646–54 (2024). https://doi.org/10.1038/s41929-024-01148-x.

11 Xu, Y., Ge, R., Yang, J., Li, J., Li, S., Li, Y., Zhang, J., Feng, J., Liu, B., and Li, W. Molybdenum disulfide (MoS2)-based electrocatalysts for hydrogen evolution reaction: From mechanism to manipulation. Journal of Energy Chemistry, 74, 45–71 (2022). https://doi.org/10.1016/j.jechem.2022.06.031.

12 Kong, L., Pan, L., Guo, H., Qiu, Y., Alshahrani, W.A., Amin, M.A., and Lin, J. Constructing WS2/WO3-x heterostructured electrocatalyst enriched with oxygen vacancies for accelerated hydrogen evolution reaction. Journal of Colloid and Interface Science, 664, 178–85 (2024). https://doi.org/10.1016/j.jcis.2024.03.002.

13 Yang, F., Pan, Y., and Zhu, J. Enhanced catalytic activity of noble metal@borophene/WS2 heterojunction for hydrogen evolution reaction. Applied Surface Science, 680, 161321 (2025). https://doi.org/10.1016/j.apsusc.2024.161321.

14 Tekalgne, M.A., Do, H.H., Nguyen, T. Van, Le, Q. Van, Hong, S.H., Ahn, S.H., and Kim, S.Y. MXene Hybrid Nanosheet of WS_2 /Ti_3C_2 for Electrocatalytic Hydrogen Evolution Reaction. ACS Omega, 8 (44), 41802–8 (2023). https://doi.org/10.1021/acsomega.3c06403.

15 Sun, R., Wang, Z., and Zhao, J. Transition metal-anchored WS2 nanosheets as efficient electrocatalysts for hydrogen evolution reaction: A first-principles study. Molecular Catalysis, 588, 115519 (2026). https://doi.org/10.1016/j.mcat.2025.115519.

16 Rahmani, E., Reyhani, A., Khanlary, M.R., Mortazavi, S.Z., Mohammadi, M.R., Dau, H., Gholami, M.F., Mohammadi, A.B., Rabe, J.P., Soleimani, M., and Zarabadipoor, M. Phosphorus doped few layer WS2 flakes grown by chemical vapor deposition for hydrogen evolution reactions. Scientific Reports, 15 (1), 6350 (2025). https://doi.org/10.1038/s41598-025-90341-4.

17 Joseph, A., Chacko, L., Sanal, K.C., Pineda-Aguilar, N., Jasna, M., Antony, A., and Aneesh, P.M. Efficient hydrogen evolution reaction performance of Ni substituted WS2 nanoflakes. Applied Physics A, 130 (12), 875 (2024). https://doi.org/10.1007/s00339-024-08050-0.

18 Nguyen, T. Van, Huynh, K.A., Le, Q. Van, Ahn, S.H., and Kim, S.Y. Facile Synthesis of WS_2 /WO_3 Materials in a Batch Reactor for the Hydrogen Evolution Reaction. International Journal of Energy Research, 2024 (1) (2024). https://doi.org/10.1155/2024/4878549.

19 Singh, T., Deepak, D., Panghal, A., and Roy, S.S. Laser-induced graphene nano-anchored WS2/WO3 heterostructures for electrocatalytic oxygen evolution reaction. International Journal of Hydrogen Energy, 84, 939–50 (2024). https://doi.org/10.1016/j.ijhydene.2024.08.272.

20 Markhabayeva, A. Synthesis of hierarchical wo3 microspheres for photoelectrochemical water splitting application. Physical Sciences and Technology, 10 (2) (2023). https://doi.org/10.26577/phst.2023.v10.i2.04.

21 Liao, L., Zhao, Y., Zhou, H., Li, D., Qi, Y., Zhang, Y., Sun, Y., Zhou, Q., and Yu, F. Edge-oriented N-Doped WS_2 Nanoparticles on Porous Co_3N Nanosheets for Efficient Alkaline Hydrogen Evolution and Nitrogenous Nucleophile Electrooxidation. Small, 18 (40) (2022). https://doi.org/10.1002/smll.202203171.

22 Huang, X., Jiang, H., Ge, B., Huang, C., and Tang, J. Nitrogen-Doped NiS/WS 2 Heterostructures on Carbon Cloth: A Synergistic Route to High-Performance Hydrogen Evolution Catalysts. ChemSusChem, 19 (11) (2026). https://doi.org/10.1002/cssc.70782.

23 Arumugam, D., Subramani, M., Subramani, D., and Ramasamy, S. Unraveling the potential of transition metals as single atom catalyst in Graphene/WS2 van der Waals heterostructure for enhanced HER performance – A first principles study. International Journal of Hydrogen Energy, 68, 545–58 (2024). https://doi.org/10.1016/j.ijhydene.2024.04.281.

24 Nasr, M., Benhamou, L., Kotbi, A., Rajput, N.S., Campos, A., Lahmar, A.-I., Hoummada, K., Kaja, K., El Marssi, M., and Jouiad, M. Photoelectrochemical Enhancement of Graphene@WS2 Nanosheets for Water Splitting Reaction. Nanomaterials, 12 (11), 1914 (2022). https://doi.org/10.3390/nano12111914.

25 Liu, F., Zeng, D., Tian, Y., Hu, Y., Shen, T., Gao, Y., and Guan, R. Ternary heterostructure Cu-ZnIn2S4/WO3/WS2 flower-like microspheres for highly-efficient photocatalytic hydrogen evolution under visible-light irradiation. Applied Surface Science, 642, 158572 (2024). https://doi.org/10.1016/j.apsusc.2023.158572.

26 Rasool, F., Pirzada, B.M., Talib, S.H., Alkhidir, T., Anjum, D.H., Mohamed, S., and Qurashi, A. In Situ Growth of Interfacially Nanoengineered 2D–2D $WS_2/Ti_3C_2T_x$ MXene for the Enhanced Performance of Hydrogen Evolution Reactions. ACS Applied Materials & Interfaces, 16 (11), 14229–42 (2024). https://doi.org/10.1021/acsami.3c11642.

27 Ladhane, S., Shah, S., Shinde, P., Punde, A., Waghmare, A., Hase, Y., Bade, B.R., Doiphode, V., Rahane, S.N., Kale, D., Rondiya, S.R., Prasad, M., Patole, S.P., and Jadkar, S.R. Enhanced Photoelectrochemical Activity Realized from WS_2 Thin Films Prepared by RF-Magnetron Sputtering for Water Splitting. ChemElectroChem, 11 (7) (2024). https://doi.org/10.1002/celc.202400002.

28 Ladhane, S., Shah, S., Doiphode, V., Shinde, P., Kale, D., Rahane, S., Thombare, J., Ingole, M., Vairale, P., Hase, Y., Waghmare, A., Prasad, M., Patole, S.P., and Jadkar, S. Pressure-dependent growth of RF-sputtered WS2 nanostructures for enhanced hydrogen production via photoelectrochemical water splitting. Journal of Power Sources, 640, 236786 (2025). https://doi.org/10.1016/j.jpowsour.2025.236786.

29 Ladhane, S., Shah, S., Doiphode, V., Shinde, P., Kale, D., Rahane, S., Thombare, J., Ingole, M., Vairale, P., Hase, Y., Waghmare, A., Prasad, M., Patole, S.P., and Jadkar, S. Tailoring CdS/WS2 heterostructures for enhanced photoelectrochemical water splitting via RF magnetron sputtering. Journal of Power Sources, 656, 238056 (2025). https://doi.org/10.1016/j.jpowsour.2025.238056.

30 Van Toan, N., Sui, H., Li, J., Tuoi, T.T.K., and Ono, T. Nanoengineered micro-supercapacitors based on graphene nanowalls for self-powered wireless sensing system. Journal of Energy Storage, 81, 110446 (2024). https://doi.org/10.1016/j.est.2024.110446.

31 Farid, G., Amade, R., Chaitoglou, S., Alshaikh, I., Ospina, R., Ma, Y., and Bertran-Serra, E. Efficient flexible electrodes for lithium-ion batteries utilizing well-dispersed hybrid Mo2C nanoparticles on vertically-oriented graphene nanowalls. Journal of Alloys and Compounds, 968, 172109 (2023). https://doi.org/10.1016/j.jallcom.2023.172109.

32 Stoian, M.C., Romanitan, C., Simionescu, O.G., Djourelov, N., Brincoveanu, O., Dinescu, A., and Radoi, A. Growth of nanocrystalline graphite and vertically aligned graphite nanowalls thin films and their transfer on flexible substrates for applications as electrochemical sensors for anthracene detection. Microchemical Journal, 207, 111828 (2024). https://doi.org/10.1016/j.microc.2024.111828.

33 Chaitoglou, S., Ospina, R., Ma, Y., Amade, R., Vendrell, X., Rodriguez-Pereira, J., and Bertran-Serra, E. Deposition and in-situ formation of nanostructured Mo2C nanoparticles on graphene nanowalls support for efficient electrocatalytic hydrogen evolution. Journal of Alloys and Compounds, 972, 172891 (2024). https://doi.org/10.1016/j.jallcom.2023.172891.

34 Zhumadilov, B.Ye., Zhumadilov, R.Ye., Nemkayeva, R.R., Markhabayeva, A.A., Ramazanov, T.S., Yerlanuly, Y., and Gabdullin, M.T. WO3-modified carbon nanowall electrodes for efficient hydrogen evolution reaction. International Journal of Hydrogen Energy, 223, 154356 (2026). https://doi.org/10.1016/j.ijhydene.2026.154356.

35 Zhumadilov, B.Y., Zhumadilov, R.Y., Nemkayeva, R.R., Markhabayeva, A.A., Bozheyev, F., Ramazanov, T.S., Yerlanuly, Y., and Gabdullin, M.T. Influence of Substrate Type and Synthesis Time on Morphological and Structural Properties of Carbon Nanowalls. Advanced Physics Research, 4 (12) (2025). https://doi.org/10.1002/apxr.202500156.

36 Madadkhani, S., Nandy, S., Chae, K.H., Aleshkevych, P., and Najafpour, M.M. Advances in Understanding Tungsten Disulfide Dynamics during the Hydrogen-Evolution Reaction: An Initial Step in Elucidating the Mechanism. The Journal of Physical Chemistry Letters, 15 (19), 5112–9 (2024). https://doi.org/10.1021/acs.jpclett.4c00924.

37 Van Nguyen, T., Tekalgne, M., Nguyen, T.P., Van Le, Q., Ahn, S.H., and Kim, S.Y. Electrocatalysts based on MoS_2 and WS_2 for hydrogen evolution reaction: An overview. Battery Energy, 2 (3) (2023). https://doi.org/10.1002/bte2.20220057.

38 Wang, R., Zhang, D., Luo, S., Wang, Q., Jiang, L., Wei, G.-F., and Wang, X. Incorporation of tungsten nanoparticles on WS2 film for the enhanced hydrogen evolution. International Journal of Hydrogen Energy, 59, 645–53 (2024). https://doi.org/10.1016/j.ijhydene.2024.02.010.

39 Shin, Y., Kim, J., Jang, Y., Ko, E., Lee, N.-S., Yoon, S., and Kim, M.H. Vertically-Oriented WS2 Nanosheets with a Few Layers and Its Raman Enhancements. Nanomaterials, 10 (9), 1847 (2020). https://doi.org/10.3390/nano10091847.

40 Rajeswaran, B., Konar, R., Yitzhari, R., Nessim, G.D., and Tischler, Y.R. Enhancement of the E^1_{2g} and A_{1g} Raman modes and layer identification of 2H-WS_2 nanosheets with metal coatings. Journal of Raman Spectroscopy, 54 (9), 1030–7 (2023). https://doi.org/10.1002/jrs.6585.

41 ZHUMADILOV, B., KENZHEGULOV, A., NEMKAYEVA, R., PARTIZAN, G., YERLANULY, Y., and GADBULLIN, M. Synthesis of carbon nanowalls by oxy-acetylene torch method. Journal of Metals, Materials and Minerals, 33 (4), 1806 (2023). https://doi.org/10.55713/jmmm.v33i4.1806.

42 Minh, N.Q., Van Nong, N., Dela Vega, M.S.D.C., Oda, O., and Hori, M. Synthesis of highly dense and multi-branched carbon nanowalls by two-step growth combining different plasma chemical vapor deposition methods. Vacuum, 213, 112118 (2023). https://doi.org/10.1016/j.vacuum.2023.112118.

[1,2*]Жумадилов Б.Е.,
докторант, ORCID ID: 0000-0001-5784-3840,
*e-mail: zhumadilovbe@gmail.com
[1,2]Мархабаева А.А.,
PhD, ORCID ID: 0000-0002-0657-422X,
e-mail: aiko_marx@mail.ru
[1,3]Габдуллин М.Т.,
PhD, ORCID ID: 0000-0003-4853-3642,
e-mail: gabdullin@physics.kz

[1]Қолданбалы ғылымдар және ақпараттық технологиялар институты, Алматы қ., Қазақстан
[2]Әл-Фараби атындағы Қазақ ұлттық университеті, Алматы қ., Қазақстан
[3]Қазақ-Британ техникалық университеті, Алматы, Қазақстан

Ti ЖӘНЕ Ti/КНҚ ТӨСЕМДЕРІНДЕ RF МАГНЕТРОНДЫ ШАШЫРАТУ АРҚЫЛЫ АЛЫНҒАН WS_2 ЖҰҚА ҚАБЫҚШАЛАРЫ: ҚҰРЫЛЫМДЫҚ СИПАТТАМА ЖӘНЕ СБР ӨНІМДІЛІГІ

Аңдатпа

Жер қыртысында мол таралған материалдарға негізделген сутегі бөліну реакциясының (СБР) электрокатализаторлары асыл металл катализаторларына перспективті балама саналады. Бұл жұмыста қабықша қалыңдығының құрылымдық және электрохимиялық қасиеттерге әсерін зерттеу мақсатында WS_2 жұқа қабықшалары RF магнетронды шашырату әдісімен титан төсемдеріне 30–120 минут аралығындағы әртүрлі шашырату уақыттарында тұндырылды. Сонымен қатар, тігінен бағытталған көміртекті наноқабырғаларды (КНҚ) WS_2 каталитикалық қабатымен біріктіру арқылы Ti/КНҚ/WS_2 композиттік электродтары дайындалды. Раман спектроскопиясының нәтижелері көпқабатты WS_2 қабықшаларының сәтті түзілгенін растады. Электрохимиялық өлшеулер СБР өнімділігінің WS_2 тұндыру уақытына тығыз байланысты екенін көрсетті. Зерттелген үлгілердің ішінде 90 минут тұндыру уақытымен дайындалған Ti/WS_2 электроды ең жоғары

каталитикалық белсенділік көрсетті: 10 мА см$^{-2}$ ток тығыздығында асқын кернеу 294 мВ-ты құрады, ал заряд тасымалдау кедергісі Ti/WS_2 сериясындағы ең төмен мәнге (Rct = 15,9 Ом) жетті. Электрохимиялық активтендіруден кейін асқын кернеу 144 мВ-қа дейін төмендеді. Электрохимиялық импеданстық спектроскопия (ЭИС) КНҚ енгізу заряд тасымалдау кинетикасын айтарлықтай жақсартып, Rct мәнін 3,7 Ом-ға дейін төмендеткенін көрсетті. Алайда электрон тасымалының жақсаруына қарамастан, Ti/КНҚ/WS_2 электроды СБР белсенділігі бойынша Ti/WS_2 электродынан жоғары нәтиже көрсетпеді. Бұл каталитикалық өнімділіктің тек заряд тасымалдау қасиеттеріне ғана емес, сонымен қатар белсенді орталықтардың тығыздығы мен қолжетімділігіне де тәуелді екенін көрсетеді. Алынған нәтижелер тиімді сутегі өндіру үшін WS_2 қабықшасының қалыңдығы мен электрод архитектурасын оңтайландырудың маңыздылығын айқындайды.

Түйін сөздер: сутегі бөліну реакциясы, вольфрам дисульфиді, RF магнетронды шашырату, көміртекті наноқабырғалар, электрокатализ, электрохимиялық импедансты спектроскопия.

[1,2*]Жумадилов Б.Е.,
докторант, ORCID ID: 0000-0001-5784-3840,
*e-mail: zhumadilovbe@gmail.com
[1,2]Мархабаева А.А.,
PhD, ORCID ID: 0000-0002-0657-422X,
e-mail: aiko_marx@mail.ru
[1,3]Габдуллин М.Т.,
PhD, ORCID ID: 0000-0003-4853-3642,
e-mail: gabdullin@physics.kz

[1]Институт прикладных наук и информационных технологий, г. Алматы, Казахстан
[2]Казахский национальный университет им. аль-Фараби, г. Алматы, Казахстан
[3]Казахстанско-Британский технический университет, г. Алматы, Казахстан

ТОНКИЕ ПЛЕНКИ WS_2, НАНЕСЕННЫЕ НА ПОДЛОЖКИ Ti И Ti/УНС МЕТОДОМ RF МАГНЕТРОННОГО РАСПЫЛЕНИЯ: СТРУКТУРНАЯ ХАРАКТЕРИЗАЦИЯ И ЭФФЕКТИВНОСТЬ РЕАКЦИИ ВЫДЕЛЕНИЯ ВОДОРОДА

Аннотация

Электрокатализаторы реакции выделения водорода (РВВ) на основе распространенных в природе материалов являются перспективной альтернативой катализаторам из благородных металлов. В данной работе тонкие пленки WS_2 были нанесены на титановые подложки методом RF магнетронного распыления при временах осаждения от 30 до 120 мин. с целью исследования влияния толщины пленки на структурные и электрохимические свойства. Кроме того, были изготовлены композитные электроды Ti/УНС/WS_2 путем сочетания вертикально ориентированных углеродных наностенок (УНС) с каталитическим слоем WS_2. Рамановская спектроскопия подтвердила успешное формирование многослойных пленок WS_2. Электрохимические измерения показали, что эффективность РВВ существенно зависит от времени осаждения WS_2. Среди исследованных образцов электрод Ti/WS_2, приготовленный при времени осаждения 90 мин., продемонстрировал наибольшую каталитическую активность: перенапряжение при плотности тока 10 мА·см$^{-2}$ составило 294 мВ, а сопротивление переносу заряда оказалось наименьшим в серии Ti/WS_2 (R_{ct} = 15,9 Ом). После электрохимической активации перенапряжение дополнительно снизилось до 144 мВ. Электрохимическая импедансная спектроскопия (ЭИС) показала, что введение УНС значительно улучшает кинетику переноса заряда, снижая R_{ct} до 3,7 Ом. Однако, несмотря на улучшенный электронный транспорт, электрод Ti/УНС/WS_2 не превзошел Ti/WS_2 по активности в РВВ, что свидетельствует о том, что каталитическая эффективность определяется не только свойствами переноса заряда, но и плотностью и доступностью активных центров. Полученные результаты подчеркивают важность оптимизации толщины пленки WS_2 и архитектуры электрода для эффективного производства водорода.

Ключевые слова: реакция выделения водорода, дисульфид вольфрама, RF магнетронное распыление, углеродные наностенки, электрокатализ, электрохимическая импедансная спектроскопия.